ACTA NEUROBIOLOGIAE EXPERIMENTALIS

Research paper Acta Neurobiol Exp 2010, 70: 147–164

Influence of pediatric vaccines on amygdala growth and opioid ligand binding in rhesus macaque infants: A pilot study

Laura Hewitson[1,2,*], Brian J. Lopresti[3], Carol Stott[4], N. Scott Mason[3] and Jaime Tomko[1]

[1]Department of Obstetrics and Gynecology, University of Pittsburgh School of Medicine, Pittsburgh, PA, USA; [2]Thoughtful House Center for Children, Austin, TX, USA; [3]Department of Radiology, University of Pittsburgh School of Medicine, Pittsburgh, PA, USA; [4]Independent Chartered Scientist, Cambridge, UK;
*Email: lch1@pitt.edu

This longitudinal, case-control pilot study examined amygdala growth in rhesus macaque infants receiving the complete US childhood vaccine schedule (1994-1999). Longitudinal structural and functional neuroimaging was undertaken to examine central effects of the vaccine regimen on the developing brain. Vaccine-exposed and saline-injected control infants underwent MRI and PET imaging at approximately 4 and 6 months of age, representing two specific timeframes within the vaccination schedule. Volumetric analyses showed that exposed animals did not undergo the maturational changes over time in amygdala volume that was observed in unexposed animals. After controlling for left amygdala volume, the binding of the opioid antagonist [^{11}C]diprenorphine (DPN) in exposed animals remained relatively constant over time, compared with unexposed animals, in which a significant decrease in [^{11}C]DPN binding occurred. These results suggest that maturational changes in amygdala volume and the binding capacity of [^{11}C]DPN in the amygdala was significantly altered in infant macaques receiving the vaccine schedule. The macaque infant is a relevant animal model in which to investigate specific environmental exposures and structural/functional neuroimaging during neurodevelopment.

Key Words: rhesus macaques, *Macaca mulatta*, non-human primates, animal model, neuroimaging, PET, MRI, amygdala, opioids, ethyl mercury, thimerosal, neurotoxicity

INTRODUCTION

The amygdala, a complexly interconnected limbic system structure located in the temporal lobe of the brain, is thought to play a central role in the expression of emotions (reviewed by Aggleton 1992). In rhesus macaques the amygdala has been associated with the development of social and emotional behavior (reviewed by Brothers 1990). When neonatal macaques received lesions to the amygdala they showed increasing socio-emotional disturbances including abnormal social interaction, absence of facial and body expression, and stereotypic behaviors (Bachevalier 1994). Amaral and colleagues reported that infant monkeys with bilateral amygdala lesions were still capable of interpreting and generating social behaviors (Prather et al. 2001) but failed to develop an appropriate fear response (Antoniadis et al. 2009), implicating an important role for the amygdala in regulating such responses (reviewed by Amaral and Corbett 2003, Amaral et al. 2008, Machado et al. 2009, Roozendaal et al. 2009). While the human amygdala has been well studied longitudinally in both normal and disease states, there is a paucity of information regarding amygdala growth during non-human primate development.

Evidence from animal model systems indicates that endogenous opioids play an important role in neural and behavioral ontogeny (Zagon et al. 1982). The primate amygdala has been shown to have a high avidity for opioids. For example, high levels of [^{3}H]diprenorphine (DPN)-binding in the amygdala of healthy adult male cynomolgus monkeys (*Macaca fascicularis*) were

Correspondence should be addressed to L. Hewitson
Email: lch1@pitt.edu

Received 1 April 2010, accepted 30 June 2010

observed when mapping opiate-receptor density by autoradiography (Wamsley et al. 1982). In addition, alterations in amygdala opioid-ligand binding is associated with toxic injury to the brain. Cohen and colleagues used high-resolution positron emission tomography (PET) to examine the long term influence of the neurotoxin 1-methyl-4-phenyl-1,2,3,6-tetrahydropyridine (MPTP) on opioid-ligand binding in adult rhesus macaques, in whom, as with humans, this agent produces a Parkinson's-like syndrome (Cohen et al. 1998). Using 6-deoxy-6-β-[^{18}F]fluoronaltrexone (Cyclofoxy, CF), a μ-and κ-opiate selective receptor antagonist radioligand, the amygdala displayed a high avidity for CF in the normal macaque, which was significantly reduced in animals treated with MPTP 4-5 years earlier. Opioid-ligand binding in the amygdalae of infant macaques during development has not been examined.

Longitudinal studies of non-human primates provides a complementary approach to clinical studies since their environment can be selectively manipulated and tightly controlled, and pre-and post-exposure testing enables the detection of deviations from normal biological and behavioral trajectories. Non-human primates are particularly useful for studying aspects of vaccine safety (Kennedy et al. 1997). In the 1990's, the majority of approved pediatric vaccines contained the preservative thimerosal, an organic mercury compound with bactericidal and fungicidal properties (Ball et al. 2001). During this time, the cumulative exposure to mercury from thimerosal in infants undergoing immunization during the first 6 months of life could exceed U.S. Environmental Protection Agency guidelines (Clements et al. 2000). Thimerosal was removed from most pediatric vaccines in the United States in 2001 (Ball et al. 2001), based on the risk assessment assumption that the dose-effect and dose-response relationships of ethylmercury, the presumed metabolite of thimerosal (Tan and Parkin 2000, Wu et al. 2008), and methylmercury were the same. The safety of the combined vaccine regimen *per se,* rather than that of individual vaccines or vaccine components, is an important aspect of vaccine safety that has not been examined. In order to more directly investigate the neurodevelopmental impact of the complete US pediatric vaccine schedule (1994-1999), our model examined structural and functional changes in the amygdala before and after vaccination in the developing infant primate brain. Longitudinal development and functional characteristics of the amygdala are reported in vaccinated (exposed) and unvaccinated (unexposed) animals, and data on the novel application of [^{11}C]DPN PET to the study of macaque central nervous system (CNS) development are presented.

METHODS

Animal Assurances

All procedures used in this research followed the guidelines of the Animal Welfare Act and the Guide for Care and Use of Laboratory Animals of the National Research Council to ensure adequate measures were taken to minimize pain and discomfort. Research protocols were approved by both the University of Pittsburgh and the Magee-Womens Research Institute and Foundation (MWRI&F) Institutional Animal Care and Use Committees (IACUC).

Animal Husbandry

The animals reported here were part of a larger comprehensive 5 year study which included neurodevelopmental, behavioral and immunological observations. Rhesus macaque (*Macaca mulatta*) infants were separated from their mothers at birth and reared in a neonatal nursery according to the published protocols (Ruppenthal and Sackett 1992). Separation was necessary for this study as mothering precludes neonatal testing due to the distress caused to both the mother and the neonate when temporarily separated (Suomi et al. 1983, Sackett et al. 2002). The only way to rigorously test neonatal behavioral development is to remove the infant from its mother at birth (Ruppenthal and Sackett 1992, Sackett et al. 2002). This protocol also permits the routine collection of blood, urine and stool samples that were required for other aspects of the study not reported here. The birth weights of all infants were within the normal range for this species. Environmental conditions were strictly controlled in the nursery to eliminate differences due to factors such as diet or infant handling. Infants were similarly isolated, housed, and raised as previously described (Hewitson et al. 2010a). Briefly, infants received a standard infant baby formula (Enfamil, Mead Johnson and Co.) with the introduction of animal biscuits containing approximately 15% wheat gluten (Purina Mills, St. Louis, MO) at approximately 1 month of age.

Nursery caging contained a cloth surrogate device and formula feeder until 21 days, when infants were re-housed in individual cages in the main rearing rooms. At 4 months of age infants were weaned from formula to water containing a bovine sodium caseinate (American Casein Company, Burlington, NJ) to maintain the dietary casein level at approximately 40%. At the same time, small pieces of fruit were introduced. All infants underwent standard cognitive assessments (not reported here) and daily social interactions within their peer group (Ruppenthal and Sackett 1992) and received standard environmental enrichment.

Study Design

For this pilot study, a total of sixteen male infant rhesus macaques (*Macaca mulatta*) were randomly allocated to either the exposed or unexposed study group in order to complete peer groups (Ruppenthal and Sackett 1992) such that each peer group contained animals from either the unexposed or exposed study group. Once a new peer group was started, new animals were assigned to this group until it consisted of 3 or 4 infants, the ages of which were less than 4 weeks apart from their peers. Peer groups were physically, but not visually, separated from each other to minimise any contact and reduce the risk of horizontal transmission of infectious agents, while maintaining the consistency of exposures to nursery staff, environment, food and water (Hewitson et al. 2010a). Four infants were assigned to the unexposed study group and received saline injections according to the schedule in Table I (although one control had to be withdrawn due to a scheduling an error). The remaining 12 infants were allocated to the exposed study group and received the complete, age-adjusted childhood vaccine regimen (Table I). We purposefully assigned a larger number of animals to the exposed group in order to optimize the chances of observing what we anticipated to be an uncommon or idiosyncratic effect.

Vaccine Dosing and Administration

The following single dose, preservative-free vaccines were purchased and thimerosal added as previously described (Hewitson et al. 2010a) in order to mimic the pediatric vaccines used between 1994-1999 (Centers for Disease Control, 1995): RECOMBIVAX

Table I

Pediatric vaccine schedule (1990's)	Birth	2 Months	4 Months	6 Months	12-18 Months	48 Months
Macaque vaccine schedule¶	Birth	2 Weeks	4 Weeks	6 Weeks	12-18 Weeks	52 Weeks
Vaccines administered (EtHg content)	HB (12.5μg)	HB (12.5μg) DTaP (25μg) Hib (25μg)	HB (12.5μg) DTaP (25μg) Hib (25μg)	DTaP (25μg) Hib (25μg)	MMR1 (0μg) DTaP (25μg) Hib (25μg)	MMR2 (0μg) DTaP (25μg)
EtHg (μg) boys	12.5	62.5	62.5	50	50	25
EtHg (μg) primates†	1.98	9.9	9.9	7.92	7.92	3.96

Macaque equivalents of dosing and timing of US Pediatric Vaccine Recommendations in the 1990's. Administered vaccines and ethyl mercury (EtHg) content: Hepatitis B (HB; Recombivax, Merck) – 1.98 μg; Diptheria, Tetanus, acellular Pertussis (DTaP; Infanrix, GlaxoSmithKline) – 3.96 μg; Haemophilus influenza B (Hib; PedvaxHIB, Merck) – 3.96 μg; and Measles-Mumps-Rubella (MMR II, Merck) – 0 μg. The vaccination schedule for infant primates was adjusted based on an approximately four-fold faster growth of macaque infants compared to humans (Burbacher et al. 2005; Ruppenthal 1989). †EtHg content for each vaccine was calculated based on a average weight ratio of approximately 6.3 for boys:primates (Ruppenthal 1989).

HB® (Merck) for the Hepatitis B (HB) vaccine; INFANRIX® (GlaxoSmithKline) for the diphtheria and tetanus toxoids and acellular pertussis (DTaP) vaccine; and Liquid PedvaxHIB® (Merck) for the haemophilus B (Hib) vaccine. The M-M-R® II (Merck) was used for the measles, mumps, rubella (MMR) vaccine, which has always been thimerosal-free. The thimerosal dose was standardized to the equivalent (μg/kg body weight) administered to a male human infant on the 5th percentile for weight. Standardization provided a clinical-exposure dose that allowed valid comparison of outcomes. Single dose vaccines were pooled and then spiked with a stock thimerosal solution and analyzed for ethyl mercury concentration using an Inductively Coupled Plasma Optical Emission Spectrometer to verify that target concentrations were achieved (Hewitson et al. 2010a). The dosed HB vaccine contained ~1.98 μg ethyl mercury per 0.5ml dose, while the dosed DTaP and Hib vaccines contained ~3.96 μg ethyl mercury. The schedule of vaccine administration was adjusted based on the approximately 4 to 1 faster growth of macaque infants (Gunderson and Sackett 1984, Ruppenthal 1989), following previously published protocols (Burbacher et al. 2005). Exposed infants received a 0.5ml intramuscular (i.m.) injection of each vaccine according to the schedule in Table I, except for MMR which was given sub-cutaneously. Unexposed infants followed the same schedule of injections as exposed infants except that each vaccine was replaced with 0.5ml saline, i.m.

Magnetic Resonance (MR) Image Acquisition

Neuroimaging studies (MR and PET) were undertaken for both exposed and unexposed animals at two time points: Time One (T1) at approximately 4 months of age and Time Two (T2) at approximately 6 months of age. At T1 exposed animals had received only thimerosal-containing vaccines equivalent to those given up to 6 months of age (Table I). At T2, vaccine exposure also included the primary MMR vaccine and an additional DTaP and Hib booster, equivalent to those vaccines given between 12-18 months of age for children following the recommended pediatric schedule (Centers for Disease Control, 1995). These timeframes for neuroimaging were chosen to determine whether the MMR may have contributed to any observed neurological features. Animals underwent MR imaging sessions on a Siemens 3T scanner at the Brain Imaging Research Center at the University of Pittsburgh. Three-dimensional (3D) T1 MPRAGE and T2 structural images were acquired using a 12cm Quadrature Birdcage coil (Nova Medical) and a Siemens 3T Allegra MRI System. A complete set of MRI data at both T1 and T2 were obtained from 9 exposed and 2 unexposed animals. The MR images were used for volumetric analyses, as well as for anatomical co-registration to the PET images of [^{11}C]DPN and anatomical guidance of volume-of-interest (VOI) definition. All image analysis was undertaken in an observer-blinded fashion. Structural MRI scans were segmented using open source NVM software (Neuromorphometrics 1998) and analyzed by the same MRI analyst for all images.

Positron Emission Tomography (PET)

Radiosynthesis of [^{11}C]DPN was conducted as described previously (Lever et al. 1987) from the precursor 3-*O*-trityl-6-*O*-desmethyl-diprenorphine (TDPN, ABX GmbH, Radeberg, Germany). The average injected dose of [^{11}C]DPN was 229±47 MBq with an average specific activity of 30.3±13.7 GBq/μmol. A complete set of PET data at both T1 and T2 were obtained from 9 exposed and 2 unexposed animals. PET imaging was performed as described previously (Tai et al. 2001) on a PET P4 scanner (Siemens Molecular Imaging, Knoxville, TN). Prior to radiotracer injection, a 15-min transmission scan was performed using a rotating 5 mCi ^{57}Co point source for attenuation correction of PET emission data (Carney et al. 2006). Following the injection of [^{11}C]DPN, PET emission data were acquired in list mode for a period of 60 min. The list-mode data were histogrammed and rebinned using the FORE algorithm. 3D Sinograms were reconstructed using 2D filtered back-projection. Corrections for scatter, radioactive decay, random coincidences, and scanner dead-time were applied. Absolute quantification of radioactivity was performed by cross calibration of the microPET system to a gamma counter using a solid 10 cm uniform phantom containing a known radioactivity concentration of fluorine-18.

Image Co-Registration and Volume-of-Interest (VOI) Determination

MR images were co-registered with [^{11}C]DPN images to provide anatomical guidance of VOI determina-

tion. Prior to the co-registration procedure, MPRAGE MR datasets were re-sampled to match the voxel dimensions of the PET images. Using the MedX software package (v.3.4.3), MR images were cropped to remove extracerebral structures, and used to establish the reference coordinate system for all subsequent PET scans acquired in each animal. The initial 20 min of the [^{11}C]DPN emission data were summed and co-registered to the reference MR image using the Normalized Mutual Information Algorithm (Maes et al. 1996, Studholme et al. 1999) implemented in the PMOD software package (v. 2.85, PMOD Technologies Ltd. Zurich, Switzerland). The dynamic [^{11}C]DPN dataset was resliced on a frame-by-frame basis using the transformation from the co-registration process. Serial PET images acquired in the same animal were co-registered to the reference MR image analogously. The quality of the registration was checked by locating common anatomical landmarks in an orthogonal viewer displaying the co-registered PET and MR images. VOIs were defined on a fused image of co-registered MR and PET image datasets using the PMOD data analysis package (Figure 1). Each VOI was defined by hand tracing either unilaterally or bilaterally on three to five contiguous image planes. VOIs were used to sample the dynamic PET datasets to yield regional time-varying measures of radioactivity concentration (time-activity curves [TACs]). Twelve VOIs were defined: brainstem (BST), amygdala (AMY), lateral thalamus (THL; includes lateral thalamic nuclei, anterior and posterior), dorsal caudate (DCD; includes dorsal and middle caudate, comprising the associative striatum), ventral caudate nucleus (VCD; includes ventral caudate, nucleus accumbens, and portions of rostral putamen, comprising the limbic striatum), putamen (PUT; limited to posterior aspects projecting to motor cortex, comprising the motor striatum), pregenual anterior cingulate gyrus (CIN), occipital cortex (OCC; primary visual and calcarine cortices), cerebellum (CER), and a basal forebrain/hypothalamus (BSF, includes high opiate-

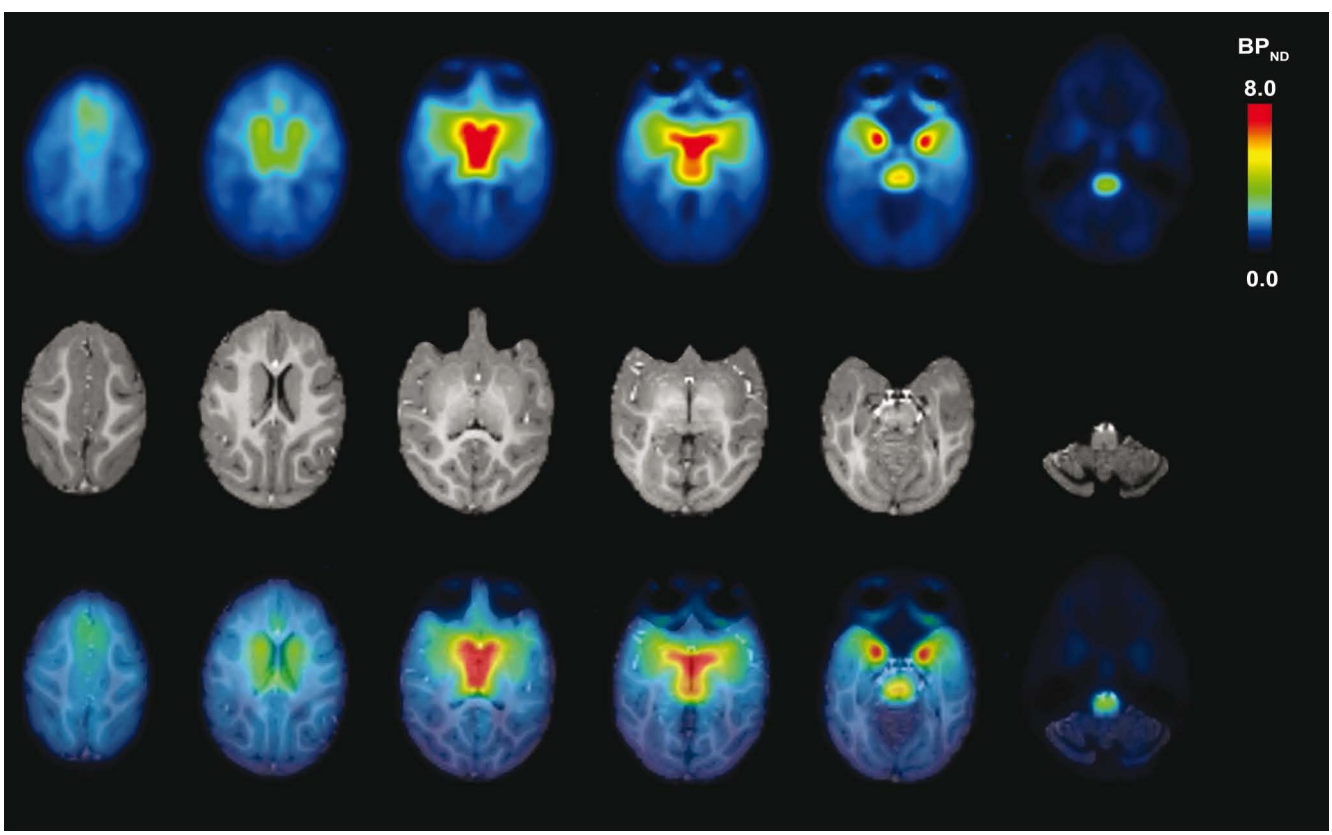

Fig. 1. Distribution of [^{11}C]DPN specific binding and MR image co-registration in a representative control infant macaque. Shown are parametric images of binding potential (BP_{ND}) at six levels through the brain (top row, superior to inferior). Also shown are corresponding slices of the animal's MR image (middle row) and a fusion of the BP_{ND} map and the MR image (bottom row).

binding structures posterior to the optic chiasm, including portions of the substantia innominata, medial and lateral preoptic area of the hypothalamus, and the horizontal and vertical diagonal bands of Broca). Only data for the amygdala are reported in this paper.

PET Data Analyses

The primary outcome measures of the PET data analyses are indices of [^{11}C]DPN-specific binding. Due to the low body mass and blood volume of the young animals used in this study (approximately 1-2 kg at T1), it was not practical to conduct conventional compartmental analyses using arterial input-function data. Rather, we employed fully image-based methods of analysis based on the definition of an anatomical "reference" region devoid of specific binding of radiotracer (Lever et al. 1987). To estimate [^{11}C]DPN-specific binding, two strategies were investigated. The first was the non-invasive Logan graphical analysis or reference Logan plot (rLP); (Logan et al. 1996), which is an extension of the earlier graphical method developed by Logan and colleagues to estimate the regional total radiotracer distribution volume (DV) for reversibly binding radiotracers (Logan et al. 1990). The rLP method was used to derive estimates of the [^{11}C]DPN distribution volume ratio (DVR) and the reference-tissue derived binding potential (BP_{ND}). Both the DVR and BP_{ND} outcome measures can be related to the free binding-site pool (B_{max}) and the ligand dissociation constant (K_D) (Innis et al. 2007).

The second method estimates radiotracer-specific binding by comparing the radioactivity concentrations between target (receptor-rich) and reference (receptor-devoid) regions (Tissue Ratio; TR). Typically, the TR is determined at steady-state kinetics, such that the ratio of radioactivity concentrations between target and reference region maintains a constant value over the selected interval. The DVR outcome is comparable to this Simple TR (target:reference), as both are indices of the ratio of total to non-specific binding. The Specific TR ([target-reference]/reference) is a more representative index of pure specific binding, which is therefore more comparable to the radiotracer BP. This method was initially validated using data from a study using [^{11}C]carfentanil, a μ-opiate selective radiotracer, and later applied to [^{11}C]DPN studies (Lever et al. 1987). Here, the 50-90 min post-injection interval most closely corresponded to the period of radiotracer steady-state, and was thus selected as the interval over which to evaluate the specific TR (TR_5090). BP_{ND} was selected as the preferred outcome measure for the rLP analyses, which was viewed to be most comparable to the specific tissue ratio outcome measure (TR_5090).

Based upon prior studies, two reference regions, cerebellar cortex (CER) and occipital cortex (OCC), were evaluated for the TR and rLP analyses. OCC has a paucity of μ-opiate receptors (Talbot et al. 2005) but contains low levels of both κ- and δ-opiate receptors (Sparks et al. 2002, Schumann et al. 2004), which would bind the non-selective opiate receptor agent [^{11}C]DPN, and therefore underestimate specific binding. Opioid receptors have also been reported in adult human cerebellum (Schadrack et al. 1999), but not in the infant macaque. In this study, the CER was consistently found to be the lowest region in terms of [^{11}C]DPN-specific binding, and therefore was the most appropriate reference region for this analysis. Data are therefore presented for CER as the reference region only.

Statistical Analysis

In light of evidence of lateralization of amygdala emotional-response patterns (Knight et al. 2005) and functional independence of right and left amygdalae (Irwin et al. 2004), the effect of exposure and time on (a) volume and (b) [^{11}C]DPN binding were undertaken separately for right, left and whole amygdalae. Analyses comprised Generalized Estimated Equation (GEE) modelling which is an extension of the General Linear Model (GLM) for longitudinal non-independent data. GEE modelling also allows evaluation of non-normally distributed data with specified link-functions (Hardin and Hilbe 2003). Normality was assessed using normality plots and the Kolmogorov-Smirnov Test, with Lilliefor's correction. GEE modelling focussed on between- and within-subject factors and covariates on repeated measures of (a) volumetric data and (b) [^{11}C]DPN binding as outcome measures. A factorial model incorporating an 'exposure by time' interaction term was generated for each anatomical region. For analyses using [^{11}C]DPN binding as outcome, the effect of volume was controlled by including mean amygdala volume (left, right or whole, as appropriate) as a covariate. Where interaction terms were significant, main effects, whether statistically significant or not, are included in

the model but are not interpreted (as per standard procedures). All GEE analyses assumed a linear model for the outcome variable, with an identity-link function. All working correlation matrices were defined as 'exchangeable'. GEE analyses provide Wald-Chi Square (χ^2) statistics for main effects and interaction terms, together with associated degrees of freedom (df) and *P* values. Pairwise contrasts of Estimated Marginal Means (EMMs) for within- and between-group comparisons generated pairwise mean differences with associated 95% Confidence Intervals (CIs), df and *P* values for the group-difference. Post-hoc comparisons used the Sequential Bonferroni correction to minimise the risk of Type One errors associated with multiple comparisons, while also minimising the reduction of power and Type Two errors associated with classic Bonferroni correction (Nakagawa 2004); df=1 in all analyses. Analyses were carried out using SPSS v.18.

The analyses involve two binary predictors – time (T1 *vs.* T2) and exposure (exposed *vs.* unexposed). A main effect of time, manifested by a significant overall difference in scores between T1 and T2 in the groups as a whole (i.e. regardless of exposure) would represent an overall maturational change with time. A main effect of exposure manifested by a significant difference in the exposed *vs.* unexposed group (regardless of time) would represent a difference between exposed and unexposed animals. An interaction effect between time and exposure, manifested by a significant time by exposure interaction term, would indicate that the effect of time is either mitigated or enhanced by expo-

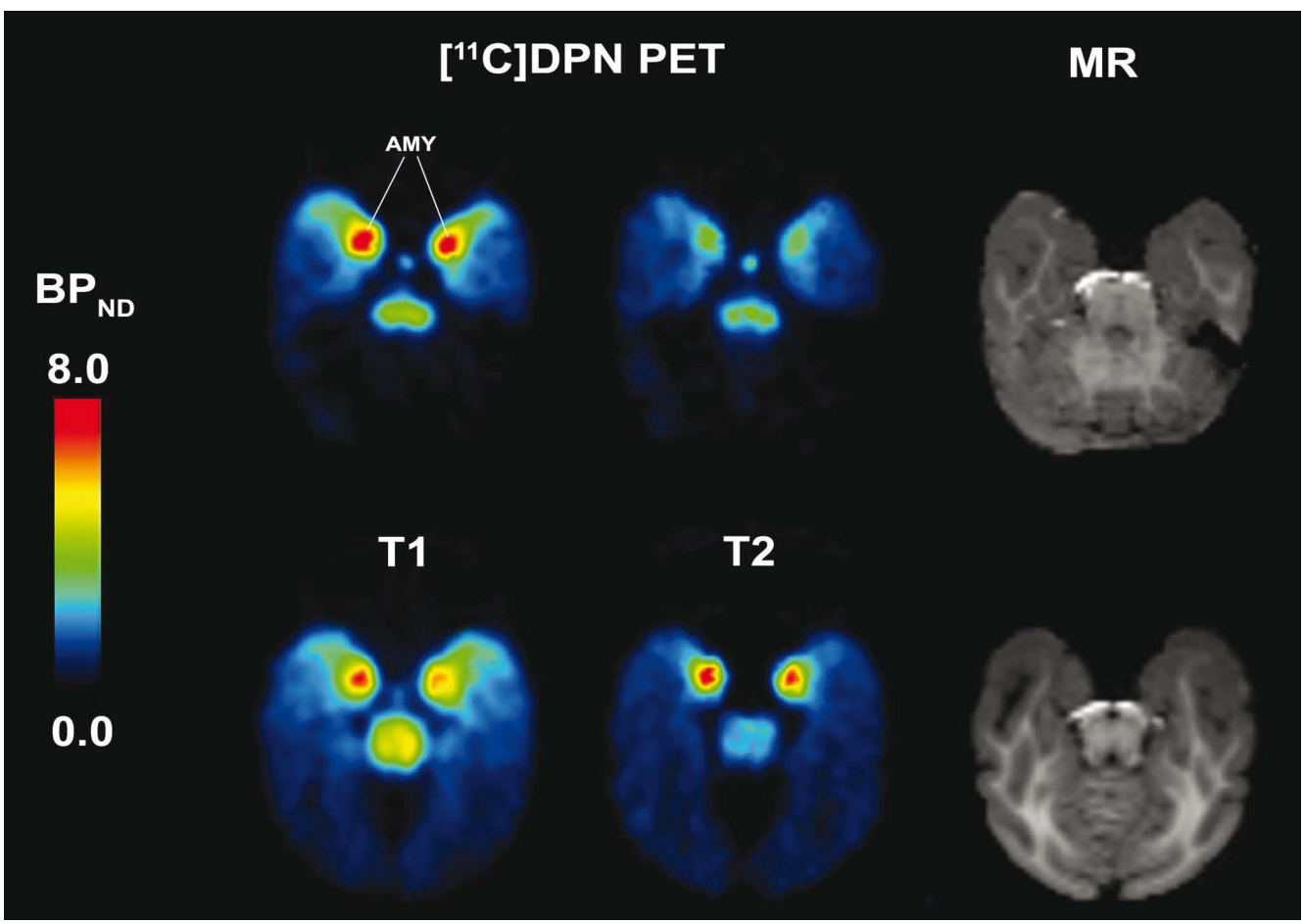

Fig. 2. Parametric images of [^{11}C]DPN-binding potential (BP_{ND}) of the amygdala. [^{11}C]DPN-binding potential (BP_{ND}) at the level of the amygdala (indicated by AMY) at Time 1 (T1; left column) and Time 2 (T2; middle column) in representative unexposed (top row) and exposed (bottom row) animals. Corresponding slices from co-registered MR images are shown for anatomical reference (right column). Maturational decline in [^{11}C]DPN-binding is seen in the unexposed animal but is not seen in the exposed animal.

sure. In other words it would indicate that the trajectory of maturational change differs between exposed and unexposed animals. In the absence of a significant interaction term, any maturational change would occur at the same rate and in the same direction, regardless of exposure. A significant interaction term would suggest that this is not the case. If for example, maturational change continues in the same direction but is significantly accelerated in one group relative to the other, or if maturational change occurs in a different direction in one group relative to the other, this would be reflected in the strength and significance of the interaction term.

In this study, outcome measurement at T1 occurs approximately 2 weeks prior to the infants receiving their scheduled vaccines at 3-4 months of age (equivalent to 12-16 months in humans; Table I) and outcome measurement at T2 occurs approximately 4-6 weeks after these vaccines are given. A significant 'interaction' term therefore suggests an effect of the vaccines given at 3-4 months of age.

RESULTS

Volumetric analyses of the total brain

GEE modelling of total brain volume as outcome, with both time (T1 vs. T2) and exposure (exposed vs. unexposed) as binary predictors revealed a significant main effect of vaccine exposure on total brain volume (Wald χ^2=4.74; P=0.029). The exposed animals had a significantly greater total brain volume independent of time (exposed *vs.* unexposed mean difference = 8020.82 mm^3; SE = 3683.38; 95% CI = 801.53 to 15240.11; P=0.029). There was no significant main effect of time (Wald χ^2=1.28; P=0.26) and no interaction between time and exposure (Wald χ^2=1.46; P=0.23). There were no significant differences within groups over time although the increase in volume between T1 and T2 for exposed animals approached significance (Table IIa) and no significant differences in total brain volume in the exposed vs. unexposed animals at either T1 or T2 (Table IIb).

Volumetric analyses of the amygdala

Total Amygdala Volume

GEE modelling with total amygdala volume as the outcome, exposure and time as factors, and total brain volume as a controlling covariate, indicated that for the exposed group there was a slight, but non-significant increase in total amygdala volume over time (P=0.81; Table IIa). In contrast, for the unexposed group there was a significant decrease in total amygdala volume over time (P<0.0001; Table IIa). There was no statistically significant difference between groups in total amylgdala volume at either time point. At T1, the mean amygdala volume in the exposed group was slightly lower than in the unexposed although not statistically significant (P=1.0; Table IIb). The difference between the groups at T2 was increased, with amygdala volume in the exposed group being higher, but not statistically significant (P=0.43; Table IIb).

Not surprisingly, given the different maturational trajectories in exposed vs. unexposed animals, (unexposed decreasing and exposed increasing) there was a statistically significant interaction between exposure and time on total amygdala volume (Wald χ^2=10.93; P=0.001). However, there were no significant main effects on total amygdala volume of either exposure (Wald χ^2=0.75; P=0.39) or time (Wald χ^2=1.14; P=0.29).

Right Amygdala Volume

As in the amygdala as a whole, after controlling for total brain volume and using time and exposure as factors, there was a statistically significant interaction between time and exposure such that the pattern of change over time in right amygdala volume differed according to exposure status (Wald χ^2=13.58; P<0.0001). For the exposed group there was a non-statistically significant increase in right amygdala volume over time (P=0.16; Table IIa). For the unexposed group there was a significant drop in right amygdala volume over time (P<0.0001; Table IIa). There were no significant main effects on right amygdala volume of either time (Wald χ^2=0.06; P=0.80) or exposure (Wald χ^2=1.11; P=0.29). There were no statistically significant differences between exposure groups in right amygdala volume at either time point. As was the case in the amygdala as a5whole, mean volume in the exposed animals at T1 was slightly lower than in the unexposed animals and the difference between the groups at T2 had increased, with volume in the exposed animals being higher, but it was not significant (T1: P=0.80; T2: P=0.18; Table IIb).

Table IIa

Within Group Differences Over Time Between Exposed and Unexposed Animals Giving Estimated Marginal Mean Differences, Standard Errors (SE) and 95% Confidence Intervals (CIs).

Volume	Exposed		Mean Difference	SE	95% Confidence Interval		P	Unexposed		Mean Difference	SE	95% Confidence Interval		P
	T1	T2			Lower	Higher		T1	T2			Lower	Higher	
Total Brain	84847.44	87476.46	-2629.03	1043.42	- 5316.71	58.65	0.06	78185.22	78097.05	88.16	1990.52	-3813.20	3989.52	0.97
Total Amy	175.79	198.80	23.00	18.00	21.96	67.97	0.81	186.62	141.29	45.15	10.17	18.33	71.93	<0.0001
Right Amy	82.82	102.09	19.28	9.00	3.92	42.47	0.16	87.68	70.83	16.85	3.88	6.62	27.08	<00001
Left Amy	92.98	96.69	3.71	11.13	- 22.93	30.35	1.00	99.50	71.17	28.33	6.47	11.26	45.40	<0.0001
Binding														
Total Amy	5.62	5.67	- 0.05	0.41	- 1.10	1.00	1.00	5.99	5.10	0.88	0.00009	0.88	0.88	<0.0001
Right Amy	5.83	5.55	0.27	0.33	- 0.58	1.13	1.00	5.80	5.65	0.15	0.0001	0.15	0.15	<0.0001
Left Amy	5.40	5.77	- 0.37	0.57	-1.84	1.10	1.00	6.11	4.64	1.46	0.46	0.26	2.66	0.008

Table IIb

Between Group Differences at Time Points One and Two Giving Estimated Marginal Mean Differences, Standard Errors (SE) and 95% Confidence Intervals (CIs)

Volume	Time One		Mean Difference	SE	95% Confidence Interval		P	Time Two		Mean Difference	SE	95% Confidence Interval		P
	Exposed	Unexposed			Lower	Higher		Exposed	Unexposed			Lower	Higher	
Total Brain	84847.44	78185.22	6662.22	3080.87	-1032.88	1432	0.12	87476.46	78097.05	9379.41	4490.91	-1837.56	20596.38	0.12
Total Amy	175.79	186.62	11.37	22.34	-38.70	61.43	1.00	199.03	141.29	56.79	33.12	-28.52	142.11	0.43
Right Amy	82.82	87.68	4.87	10.89	19.53	29.27	0.80	102.09	70.83	31.26	15.58	-7.67	70.18	0.18
Left Amy	92.98	99.50	6.51	12.71	-23.91	36.93	1.000	92.98	71.17	25.53	18.35	-21.74	72.79	0.82
Binding														
Total Amy	5.61	5.99	-0.37	1.07	-3.12	2.38	1.00	5.67	5.10	0.56	1.11	-2.27	3.39	1.00
Right Amy	5.82	5.80	0.03	1.26	-3.20	3.26	1.00	5.55	5.65	-0.95	1.20	-3.20	3.01	1.00
Left Amy	5.40	6.11	0.71	0.92	1.66	-3.08	1.00	5.77	4.65	1.12	1.07	-1.63	3.89	1.00

Left Amygdala Volume

For the exposed animals there was an increase in left amygdala volume over time, although this was not statistically significant (P=1.0; Table IIa). In contrast, for the unexposed animals there was a significant decrease in left amygdala volume from T1 to T2 (P<0.0001; Table IIa). As was the case in the amygdala as a whole, and in the right amygdala, mean volume in the exposed animals at T1 was slightly lower than in the unexposed animals and the magnitude of this difference at T2 had increased, with volume in the exposed animals being greater, but still not significantly so (T1: P=1.0; T2: P=0.82; Table IIb).

Overall, these data indicate that there was a statistically significant interaction between time and exposure on left amygdala volume, such that the pattern of change over time differed according to exposure (Wald χ^2=6.29; P=0.01). While there was no significant main effect of exposure on left amygdala volume (Wald χ^2=0.43; P=0.51), the main effect of time approached significance (Wald χ^2=3.61; P=0.06).

PET data analyses of region-specific [^{11}C]DPN-binding in macaque brain

[^{11}C]DPN was found to readily enter the infant primate brain (Figure 1) and to distribute in a manner that was consistent with specific radiotracer binding, and the known distribution of opiate receptors in the primate brain (Wamsley et al. 1982). CER was consistently the lowest region in terms of [^{11}C]DPN retention and therefore the most appropriate reference tissue. TRs determined 50-90 min post-injection approached a constant value in regions of low-to-mid receptor density, but sometimes failed to reach a plateau in regions of high receptor-density. This may be attributable to the effects of anesthesia, which may slow metabolism and result in slower radiotracer clearance. It was anticipated that the TR_5090 measures would underestimate specific binding in regions with high opioid-receptor density. While the application of the rLP method has not been previously reported for [^{11}C]DPN, here the linearity condition was consistently met in all regions (r^2>0.98). BP_{ND} values determined using rLP with CER as reference (rLP_{CER}) were found to be comparable to those determined in prior compartmental analyses of [^{11}C]DPN in humans (Sadzot et al. 1991, Schadrack et al. 1999).

In general, all measures of specific binding showed a similar rank order in their respective specific-binding measures. The regions found to possess the highest specific binding of [^{11}C]DPN were consistently the chiasmatic area, the medial thalamus, and amygdala. The brainstem, striatal regions (VCD, DCD, PUT), and lateral thalamus were intermediate,

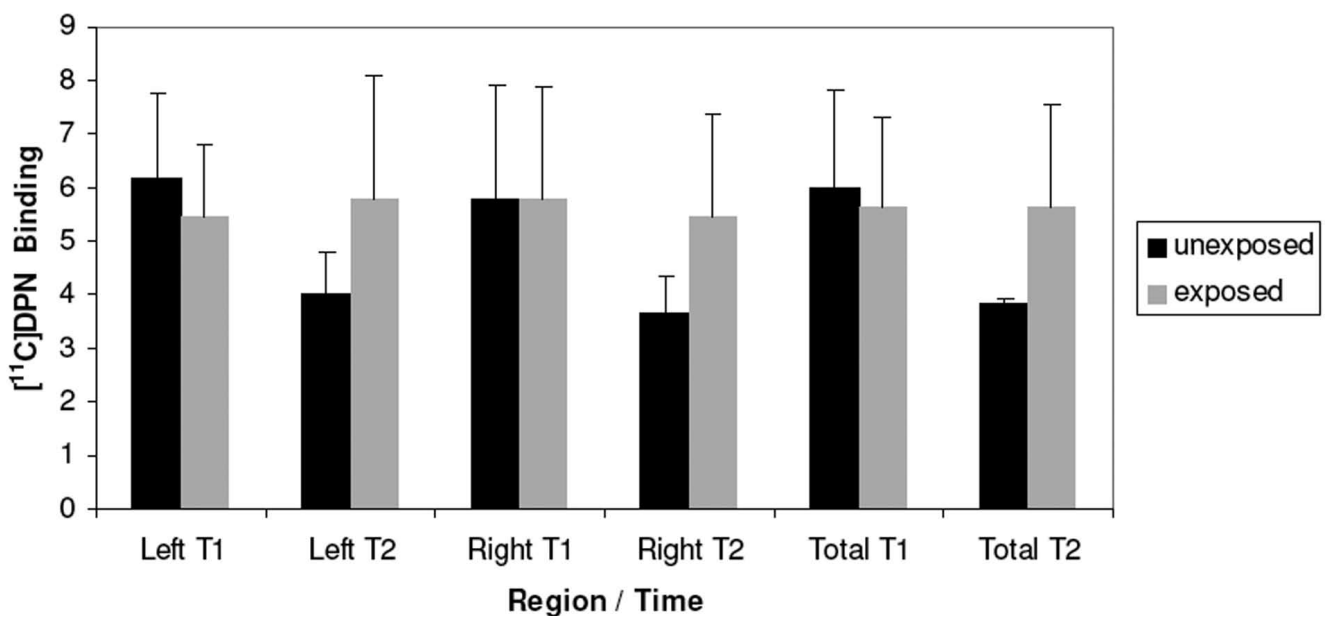

Fig. 3. [^{11}C]DPN binding potential(BP_{ND})values in the amygdalae. [^{11}C]DPN binding potential (BP_{ND}) values (raw mean+1 SD) in left, right and total amygdalae at T1 and T2 in exposed and unexposed animals determined using the Logan Reference Plot and the cerebellar cortex reference region rLP(CER).

while the frontal cortex and cingulate showed the lowest levels of [^{11}C]DPN-specific binding. In general, the use of OCC as reference yielded a bias towards lower indices of specific binding for both the rLP and TR_5090 analyses, likely due to a small component of specific binding present in OCC. While the methods produced outcomes that were highly correlated, regardless of which reference tissue was selected (CER or OCC), the TR-based methods were more variable than the rLP methods (Table III). Overall, therefore, the rLP_{CER} BP outcome measure was determined to be superior in terms of bias and variability, and analyses below are presented for this method. No correlation between the specific binding measures in any brain region and the injected mass or injected mass per kg of diprenorphine was observed, suggesting that variations in the *in vivo*-specific-binding [^{11}C]DPN were unrelated to the carrier mass of diprenorphine in the radiopharmaceutical injectate.

Table III

Method		DCD	VCD	PUT	LT	MT	FC	AC	BSM	AMY	BF
rLP (CER)*	M	2.97	4.49	2.29	3.08	6.19	1.43	2.32	4.72	5.69	7.03
	SD	0.84	1.04	0.53	0.98	1.3	0.6	0.71	1.03	1.62	1.85
	CV (%)	28.3	23.2	23	32	20.9	42.1	30.8	21.7	28.5	26.3
rLP (OCC)*	mean	1.53	2.36	1.11	1.54	3.41	0.5	1.06	2.49	2.94	3.75
	std. dev	0.57	0.75	0.38	0.69	1.17	0.15	0.23	0.74	1.2	1.53
	CV (%)	37.7	31.9	34.5	44.8	34.2	30	21.5	29.7	40.8	40.7
TR_5090 (CER)*	mean	3.9	5.51	2.98	4.02	7.3	1.92	3.06	5.84	6.0	7.38
	std. dev	1.07	1.47	0.78	1.51	2.26	0.74	0.97	1.41	2.09	2.61
	CV (%)	27.4	26.8	26.2	37.4	30.9	38.7	31.7	24.1	34.8	35.3
TR_5090 (OCC)*	mean	1.89	2.83	1.33	1.94	3.9	0.66	1.33	3.02	3.17	4
	std. dev	0.74	0.97	0.48	0.91	1.54	0.2	0.33	0.96	1.47	1.93
	CV (%)	39.1	34.2	36.2	46.8	39.4	29.9	24.9	31.8	46.5	48.1

Baseline PET Imaging Outcome Measures for All Animals.*Outcome measures represents non-displaceable binding potential (BP_{ND}) computed from direct estimation of the distribution volume ratio (DVR), such that BP_{ND} = DVR –1, measured by reference Logan plot (rLP) and tissue ratio (TR). Structures: (CER) Cerebellum; (OCC) Occipital Cortex; (DCD) Dorsal Caudate; (VCD) Ventral Caudate; (PUT) Putamen; (LT) Lateral Thalamus; (MT) Medial Thalamus; (FC) Frontal Cortex; (AC) Anterior Cingulate: (BSM) Brainstem; (AMY) Amygdala; (BSF) Basal Forebrain.

[^{11}C]DPN binding is influenced by vaccine exposure and amygdala volume

GEE analyses evaluating the impact of vaccine exposure on overall [^{11}C]DPN-binding over time, whilst controlling for amygdala volume, revealed a number of significant observations. In exposed animals, mean [^{11}C]DPN binding remained relatively stable over time compared with unexposed animals, which exhibited a maturational decrease in [^{11}C]DPN binding (Figure 3). Figure 4 shows left (A) and right (B) amygdala volume, together with left (C) and right (D) amygdala binding, by time and exposure. Interactions between variables are shown by non-parallel lines on the interaction graphs. Whether the interaction is statistically significant depends on the degree to which the lines are non-parallel. Figures 4A-C illustrate significant interactions between time and exposure for left and right amygdala volume (A-B) and for left amygdala binding (C), indicating that maturational effects operate differently in exposed vs. unexposed animals with regard to volumetric change in the amygdala as a whole, and with regard to [^{11}C]DPN binding in the left amygdala alone.

Total Amygdala [^{11}C]DPN Binding

For the total amygdala there was no main effect of time (Wald χ2=0.98; P=0.32) or exposure (Wald χ^2=0.001; P=0.97) on [^{11}C]DPN binding, and no significant interaction between time and exposure (Wald χ^2=0.78; P=0.38). The data do indicate a differential lateral effect of time according to exposure status on [^{11}C]DPN binding which is best described by considering the left and right amygdala separately below).

Left Amygdala [^{11}C]DPN Binding

There was a significant interaction between time and exposure on [^{11}C]DPN binding in the left amygdala (Wald χ^2=11.82; P=0.001). This indicates that, after controlling for left amygdala volume and the independent effects of time and exposure, the pattern and degree of change over time in [^{11}C]DPN binding in the left amygdala varied according to exposure status. In the unexposed group there was a significant decrease over time (P=0.008; Table IIa). In contrast, in the exposed group there was a non-significant increase over time, (P=1.0). No other pairwise differences approached significance either within or between groups (P=1.0; Table IIa and b). For the left amygdala there was no main effect on [^{11}C]DPN binding of either time (Wald χ^2=1.52; P=0.22) or exposure (Wald χ^2=0.05; P=0.83).

Right Amygdala [^{11}C]DPN Binding

For the right amygdala there was no main effect of either time (Wald χ^2=1.83; P=0.18) or exposure (Wald χ^2<0.0001; P=1.0) on [^{11}C]DPN binding, and no significant interaction between time and exposure (Wald χ^2=0.04; P=0.84) with a decrease in both exposed (P=1.0) and unexposed (P=0.0001) groups. While the decrease was statistically significant in the unexposed group, the concomitant decrease in the exposed group meant that the maturational trajectory of binding was not significantly different between the groups (Table IIa).

In summary, at T1 there was a significant effect of exposure on total brain volume (exposed > unexposed), but no difference in amygdala volume between groups. Changes occurring between T1 and T2 include a differential change in total amygdala volume between groups (a significant decrease in unexposed animals compared with a non-significant increase in exposed animals) after adjustment for total brain volume, and an increase in [^{11}C]DPN binding in left amygdala compared with a decrease in binding in unexposed animals, after adjusting for amygdala volume.

DISCUSSION

The structural and functional CNS alterations identified here provide a model to study the impact of early environmental exposures on primate neurodevelopment. While, as a pilot study, the size of the study groups limits the strength of the conclusions that can be drawn, the use of statistical modeling and repeated measures contributed to the study's power and increased the accuracy of the estimates. Volumetric analyses identified significantly greater total brain volume in exposed compared with unexposed animals at both measured time points. These results raise the possibility that multiple vaccine exposures during the previous 3-4 months may have had a significant impact on brain growth and development. However, for the amygdala, volumetric and

[^{11}C]DPN binding differences between groups appeared to be a function of more recent vaccine exposures, the primary MMR vaccine and the DTaP and Hib boosters given between T1 and T2. The functional observations on the differential avidity of the amygdala for [^{11}C]DPN after vaccine exposure are novel and require further study.

Interestingly, a rapid increase in total brain volume between 6 and 14 months is generally considered to be a consistent finding for many children with an Autism Spectrum Disorder (ASD) (Piven et al. 1995, Courchesne et al. 2001, Sparks et al. 2002), although this effect may be age-related (Courchesne et al. 2001, Aylward et al. 2002) and cannot be used as a biomarker for the disor-

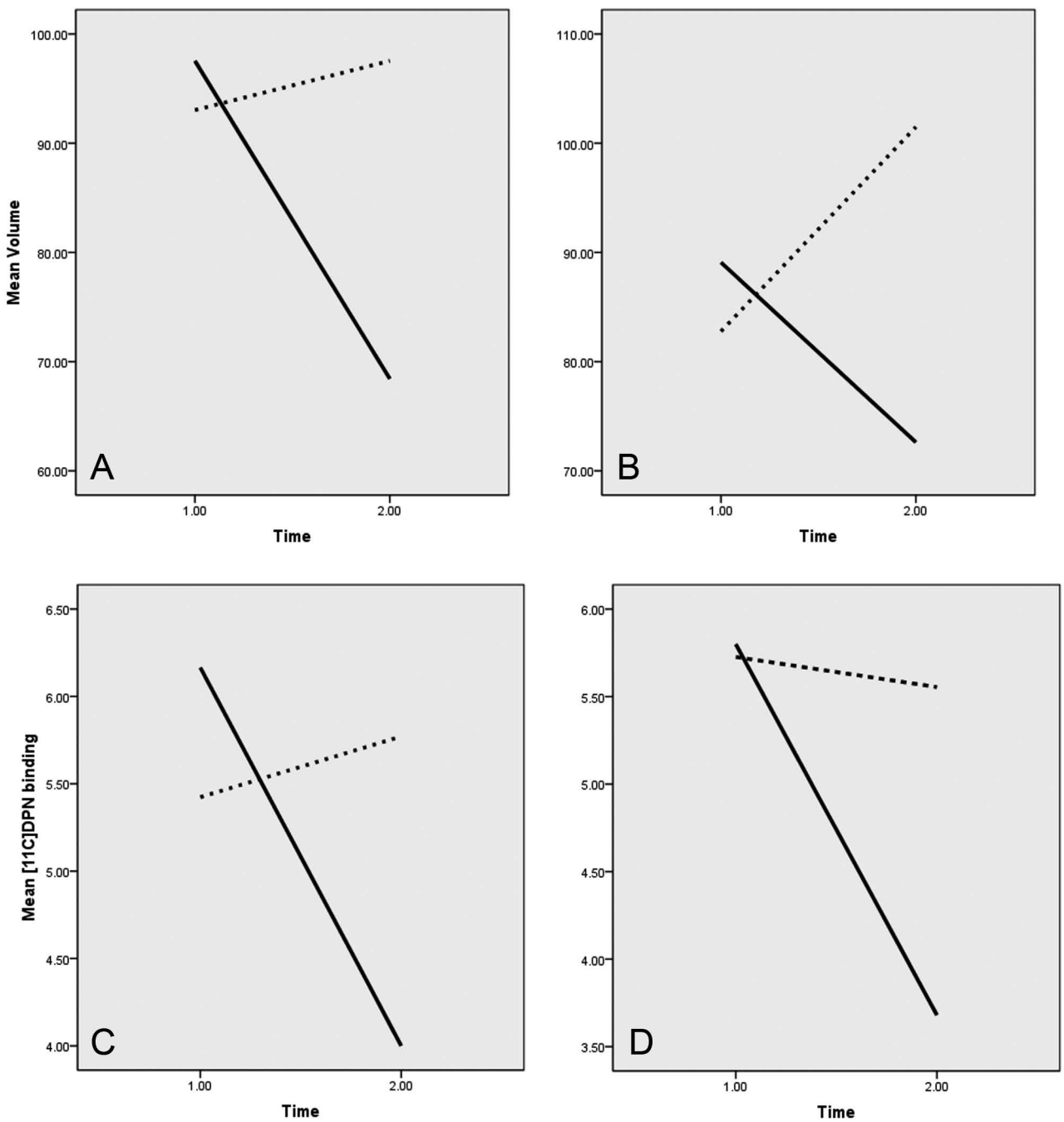

Fig. 4. Raw mean values; interaction charts of time by exposure in volume (A-B) and binding (C-D) for the left (A, C) and right (B, D) amygdala. Exposed animals represented by a dashed line; Unexposed animals represented by a solid line.

der (Herbert 2005). An enlarged brain volume may be due to a failure in programmed cell death or 'neuronal pruning', a process which rids the brain of abnormally functioning neural connections and optimizes coordinated neural functioning (Huttenlocher and Dabholkar 1997). When pruning fails to function, as may be the case in ASD, brain size will increase and neural connectivity will be decreased (Hill and Frith 2003).

Neuropathological and neuroimaging studies of individuals with an ASD, a condition in which social functioning is often severely impaired (Schultz 2005), have provided growing evidence of a central role for the amygdala (Amaral et al. 2008, Kleinhans et al. 2009). Cross-sectional studies that have stratified individuals with ASD by age and behavioral phenotype have shown that the amygdala is enlarged in younger children compared with neurotypical controls, rapidly achieves adult size in childhood, and therefore does not undergo the growth pattern observed during normal male adolescence (Schumann et al. 2004). Several studies have also demonstrated an increase in amygdala volume in young children, with the amygdala typically enlarged by approximately 15% relative to age-matched control subjects (Sparks et al. 2002, Schumann et al. 2004, Mosconi et al. 2009, Schumann et al. 2009). In the present study, amygdala volumes were significantly increased in the vaccine exposed animals relative to the unexposed animals at T2.

The data suggest that vaccine exposure may be associated with significant disturbances in central opioidergic pathways in this model. An important role for opioid ligand–receptor interactions in neuro-ontogeny and behavior is recognized during pre- and post-natal development (Zagon and McLaughlin 1985). It has been proposed that the presence of endorphines and exorphines - the latter of dietary origin - may contribute to some behavioral symptoms reported in ASD (Reichelt et al. 1981, Gillberg 1995). Neonatal assessments of this same cohort of primates previously identified significant delays in the acquisition of neonatal reflexes (Hewitson et al. 2010a) and behavioral deficits in tests of cognitive function between 5-8 months of age (Hewitson et al. 2010b) in exposed animals when compared with controls. However, the complexity of these interactions limits any inferences with respect to the precise relationship between structural and functional changes in the amygdala and the previously reported neurodevelopmental and neurobehavioral differences.

With respect to maturational changes in the amygdala, there is substantial evidence of a central role for endogenous opioid systems in regulating the structural development of the nervous system, with reported effects upon cellular proliferation, migration, differentiation, and growth (reviewed by Zagon et al. 1982). The majority of these findings have come from the experimental administration of opioid antagonists to rats during critical phases of brain development. The observed effects were dependent on dose and duration of receptor-antagonist interaction, with paradoxical effects of sustained opioid receptor blockade compared with temporary blockade, underscoring the complexity of the developing central nervous system. Maturational changes seen in the experimental setting may be relevant to the observed decline in [^{11}C]DPN-binding in the unexposed animals over time. In rats, [MET5]-enkephalin, β-endorphin, and opioid-receptor levels in the cerebellum reached their highest level in the first few weeks post-partum, and subsequently declined to low levels (Tsang et al. 1982, Zagon and McLaughlin 2004). Others have demonstrated a significant 2- to 4-fold decrease in the concentration of opiate receptors in human fetal brain tissue during the last trimester of pregnancy (Kinney et al. 1990). This may be attributable to a normal process of programmed neuronal apoptosis that can extend into infancy, and is consistent with the enlarged amygdala volume and [^{11}C]DPN-binding in exposed animals over time that was observed here.

The absence of significant change in amygdala [^{11}C] DPN binding in exposed animals over time may be attributable to a number of factors. These include the maintenance of a relatively constant absolute number of receptors, an increased occupancy of a reduced number of receptors due to an increase in endogenous and/or exogenous opioid ligands, or an increase in receptor avidity. Receptor avidity is not a direct measure of opioid receptor density, but rather a measure of both the intrinsic binding-constant and the number of unoccupied opioid receptors (Cohen et al. 1998) and thus, the results might reflect both direct and indirect effects on opioid receptor occupancy. The dynamics of any interaction of this exorphine with amygdala receptors might be relevant to the current findings. Interestingly, a recent report by Hume and colleagues showed the *in vivo* binding of [^{11}C] DPN to be insensitive to competition by acute pharmacologic doses of several potent opiate agonists, such as oxycodone (μ- and κ-opiate) and morphine (μ-opiate), but extremely sensitive to buprenorphine (~90% reduction in [^{11}C]DPN binding), which is a partial agonist of the μ-opioid receptor and an antagonist of the κ and δ opioid

receptors (Hume et al. 2007). Chronic administration of opioid antagonists has been reported to increase central opioid receptors (Van Bockstaele et al. 2006). If, for example, exorphines such as β-caseomorphine have a role in this model, either acting as partial or selective antagonists, or they exert a negative effect on endogenous opioidergic systems (LaBella et al. 1985), they might inhibit a maturational decline in opioid receptors and account for the sustained avidity of the amygdala for [^{11}C] DPN in exposed animals. How these effects could be potentially mediated by vaccine exposure is not known. Additional histologic and molecular analyses of the amygdala may provide mechanistic insights.

CONCLUSIONS

In this pilot study, infant macaques receiving the recommended pediatric vaccine regimen from the 1990's displayed a different pattern of maturational changes in amygdala volume and differences in amygdala-binding of [^{11}C]DPN following the MMR/DTaP/Hib vaccinations between T1 and T2 compared with non-exposed animals. There was also evidence of greater total brain volume in the exposed group prior to these vaccinations suggesting a possible effect of previous vaccinations to which these animals had been exposed. Because primate testing is an important aspect of pre-clinical vaccine safety assessment prior to approval for human use (Kennedy et al. 1997), the results of this pilot study warrant additional research into the potential impact of an interaction between the MMR and thimerosal-containing vaccines on brain structure and function. Additional studies are underway in the primate model to investigate the mechanistic basis for this apparent interaction.

ACKNOWLEDGEMENTS

We thank Drs. Saverio Capuano and Mario Rodriguez for veterinary assistance; and Dr. David Atwood, Carrie Redinger, Dave McFarland, Amanda Dettmer, Steven Kendro, Nicole DeBlasio, Melanie O'Malley and Megan Rufle for technical support. Special thanks to Dr. Andrew Wakefield for assistance with study design and for critical review of this manuscript; and to Troy and Charlie Ball and Robert Sawyer. This work was supported by the Johnson Family, SafeMinds, The Ted Lindsay Foundation, the Autism Research Institute, the Greater Milwaukee Foundation, the late Liz Birt, David and Cindy Emminger, Sandy McInnis, and Elyse Roberts.

REFERENCES

Aggleton JP (1992) The amygdala: neurobiological aspects of emotion, memory and mental dysfunction. Wiley–Liss, New York, NY, USA.

Amaral DG, Corbett BA (2003) The amygdala, autism and anxiety. In: Autism: neural basis and treatment possibilities. Novartis Foundation Symposium 251, June 18– 20, 2002 (Bock G, Goode J; eds.). Wiley, London, UK. p. 177–197.

Amaral DG, Schumann CM, Nordahl CW (2008) Neuroanatomy of autism. Trends Neurosci 31: 137–45.

Antoniadis EA, Winslow JT, Davis M, Amaral DG (2009) The nonhuman primate amygdala is necessary for the acquisition but not the retention of fear-potentiated startle. Biol Psychiatry 65: 241–248.

Aylward EH, Minshew NJ, Field K, Sparks BF, Singh N (2002) Effects of age on brain volume and head circumference in autism. Neurology 59: 175–183.

Bachevalier J (1994) Medial temporal lobe structures and autism: a review of clinical and experimental findings. Neuropsychologia 32: 627–648.

Ball LK, Ball R, Pratt RD (2001) An assessment of thimerosal use in childhood vaccines. Pediatrics 107: 1147–1154.

Brothers L (1990) The social brain: A project for integrating primate behaviour and neurophysiology in a new domain. Concepts Neurosci 1: 27–51.

Burbacher TM, Shen DD, Liberato N, Grant KS, Cernichiari E, Clarkson T (2005) Comparison of blood and brain mercury levels in infant monkeys exposed to methylmercury or vaccines containing thimerosal. Environ Health Perspect 113: 1015–1021.

Carney JPJ, Laymon CM, Lopresti BJ (2006) Comparison of Singles-Mode Transmission Imaging on a microPET P4 Tomograph Using Co-57 and Ge-68 Sources. IEEE Nuclear Science Symposium and Medical Imaging Conference, San Diego, CA, USA.

Centers for Disease Control [CDC] (1995). Recommended childhood immunization schedule. Morbidity and mortality weekly report (MMWR) 43: 959–950.

Clements CJ, Ball LK, Ball R, Pratt RD (2000) Thiomersal in vaccines. Lancet 355:1279–1280.

Cohen RM, Carson RE, Aigner TG, Doudet DJ (1998) Opiate receptor avidity is reduced in non-motor impaired MPTP-lesioned rhesus monkeys. Brain Res 806: 292–296.

Courchesne E, Karns CM, Davis HR, Ziccardi R, Carper RA, Tigue ZD, Chisum HJ, Moses P, Pierce K, Lord C, Lincoln AJ, Pizzo S, Schreibman L, Haas RH, Akshoomoff NA, Courchesne RY (2001) Unusual brain growth pat-

terns in early life in patients with autistic disorder: an MRI study. Neurology 57: 245–254.

Gillberg C (1995) Endogenous opioids and opiate antagonists in autism: brief review of empirical findings and implications for clinicians. Dev Med Child Neurol 37: 239–245.

Gunderson V, Sackett G (1984) Development of pattern recognition in infant pigtailed macaques (*Macaca nemestrina*). Develop Psychol 20: 412–426.

Hardin JW, Hilbe JM (2003) Generalized estimating equations. Chapman and Hall CRC, London, New York, Washington DC, USA.

Herbert MR (2005) Large brains in autism: the challenge of pervasive abnormality. Neuroscientist 11: 417–440.

Hewitson L, Houser L, Stott C, Sackett G, Tomko J, Atwood D, Blue L, White ER (2010a) Delayed acquisition of neonatal reflexes in newborn primates receiving a thimerosal-containing hepatitis B vaccine: Influences of gestational age and birth weight. J Toxic Environ Health Part A; DOI: 10.1080/15287394.2010.484709.

Hewitson L, Houser L, Sackett G, Stott C, Tomko J (2010b). Longitudinal cognitive development in rhesus infant macaques in response to vaccination: A pilot study, submitted.

Hill EL, Frith U (2003). Understanding autism: insights from mind and brain. Phil Trans R Soc Lond B 358: 281–289.

Hume SP, Lingford-Hughes AR, Nataf V, Hirani E, Ahmad R, Davies AN, Nutt DJ (2007) Low sensitivity of the positron emission tomography ligand [11C]diprenorphine to agonist opiates. J Pharmacol Exp Ther 322: 661–667.

Huttenlocher PR, Dabholkar AS (1997). Regional differences in synaptogenesis in human cerebral cortex. J Comp Neurol 387: 167–178.

Innis RB, Cunningham VJ, Delforge J, Fujita M, Gjedde A, Gunn RN, Holden J, Houle S, Huang SC, Ichise M, Iida H, Ito H, Kimura Y, Koeppe RA, Knudsen GM, Knuuti J, Lammertsma AA, Laruelle M, Logan J, Maguire RP, Mintun MA, Morris ED, Parsey R, Price JC, Slifstein M, Sossi V, Suhara T, Votaw JR, Wong DF, Carson RE (2007) Consensus nomenclature for *in vivo* imaging of reversibly binding radioligands. J Cereb Blood Flow Metab 27: 1533–1539.

Irwin W, Anderle MJ, Abercrombie HC, Schaefer SM, Kalin NH, Davidson RJ (2004) Amygdalar interhemispheric functional connectivity differs between the non-depressed and depressed human brain. Neuroimage 21: 674–686.

Kennedy RC, Shearer MH, Hildebrand W (1997) Nonhuman primate models to evaluate vaccine safety and immunogenicity. Vaccine 15: 903–908.

Kinney HC, Ottoson CK, White WF (1990) Three-dimensional distribution of 3H-naloxone binding to opiate receptors in the human fetal and infant brainstem. J Comp Neurol 291: 55–78.

Kleinhans NM, Johnson LC, Richards T, Mahurin R, Greenson J, Dawson G, Aylward E (2009) Reduced neural habituation in the amygdala and social impairments in autism spectrum disorders. Am J Psychiatry 166: 467–475.

Knight DC, Nguyen HT, Bandettini PA (2005) The role of the human amygdala in the production of conditioned fear responses. Neuroimage 26: 1193–1200.

LaBella FS, Geiger JD, Glavin GB (1985) Administered peptides inhibit the degradation of endogenous peptides. The dilemma of distinguishing direct from indirect effects. Peptides 6: 645–660.

Lever JR, Dannals RF, Wilson AA, Ravert HT, Wagner HNJ (1987) Synthesis of carbon-11 labeled diprenorphine: a radioligand for positron emission tomographic studies of opiate receptors. Tetrahedron Lett 28: 4015–4018.

Logan J, Fowler JS, Volkow ND, Wolf AP, Dewey SL, Schlyer DJ, MacGregor RR, Hitzemann R, Bendriem B, Gatley SJ (1990) Graphical analysis of reversible radioligand binding from time-activity measurements applied to [N-11C-methyl]-(-)-cocaine PET studies in human subjects. J Cereb Blood Flow Metab 10: 740–747.

Logan J, Fowler JS, Volkow ND, Wang GJ, Ding YS, Alexoff DL (1996) Distribution volume ratios without blood sampling from graphical analysis of PET data. J Cereb Blood Flow Metab 16: 834–840.

Machado CJ, Kazama AM, Bachevalier J (2009) Impact of amygdala, orbital frontal, or hippocampal lesions on threat avoidance and emotional reactivity in nonhuman primates. Emotion 9: 147–163.

Maes F, Collignon A, Vandermeulen D, Marchal G, Suetens P (1996) Multimodality image registration by maximization of mutual information. Workshop on Mathematical Methods in Biomedical Image Analysis, San Francisco, CA, USA.

Mosconi MW, Cody-Hazlett H, Poe MD, Gerig G, Gimpel-Smith R, Piven J (2009) Longitudinal study of amygdala volume and joint attention in 2- to 4-year-old children with autism. Arch Gen Psychiatry 66: 509–516.

Nakagawa SA (2004) Farewell to Bonferroni: the problems of low statistical power and publication bias. Behav Ecol 15: 1044–1045.

Neuromorphometrics (1998) Quantitative measurements in MR brain images: brain segmentation in MRI. Neuromorphometrics Inc., Somerville, MA, USA.

Piven J, Arndt S, Bailey J, Havercamp S, Andreasen NC, Palmer P (1995) An MRI study of brain size in autism. Am J Psychiatry 152: 1145–1149.

Prather MD, Lavenex P, Mauldin-Jourdain ML, Mason WA, Capitanio JP, Mendoza SP, Amaral DG (2001) Increased social fear and decreased fear of objects in monkeys with neonatal amygdala lesions. Neuroscience 106: 653–8.

Reichelt KL, Hole K, Hamberger A, Saelid G, Edminson PD, Braestrup CB, Lingjaerde O, Ledaal P, Orbeck H (1981) Biologically active peptide-containing fractions in schizophrenia and childhood autism. Adv Biochem Psychopharmacol 28: 627–643.

Roozendaal B, McEwen BS, Chattarji S (2009) Stress, memory and the amygdala. Nat Rev Neurosci 10: 423–433.

Ruppenthal GC (1989) Weight gain and intake requirements in nursery-reared macaques. In: Proc. 4th Ann Dr. Scholl Conference on the Nutrition of Captive Wild Animals (Meehan TP, Allen ME, eds.). Lincoln Park Zoological Society, Chicago, p. 20–35.

Ruppenthal GC, Sackett GP (1992) Research Protocol and Technician's Manual. Infant Primate Research Laboratory, University of Washington, Seattle, WA, USA.

Sackett GP, Ruppenthal GC, Davis AE (2002). Survival, growth, health, and reproduction following nursery rearing compared with mother rearing in pigtailed monkeys (*Macaca nemestrina*). Am J Primatol 56: 165–183.

Sadzot B, Price JC, Mayberg HS, Douglass KH, Dannals RF, Lever JR, Ravert HT, Wilson AA, Wagner HN Jr, Feldman MA (1991) Quantification of human opiate receptor concentration and affinity using high and low specific activity [11C]diprenorphine and positron emission tomography. J Cereb Blood Flow Metab 11: 204–219.

Schadrack J, Willoch F, Platzer S, Bartenstein P, Mahal B, Dworzak D, Wester HJ, Zieglgänsberger W, Tölle TR (1999) Opioid receptors in the human cerebellum: evidence from [11C]diprenorphine PET, mRNA expression and autoradiography. Neuroreport 10: 619–624.

Schultz RT (2005) Developmental deficits in social perception in autism: the role of the amygdala and fusiform face area. Int J Dev Neurosci 23: 125–141.

Schumann CM, Hamstra J, Goodlin-Jones BL, Lotspeich LJ, Kwon H, Buonocore MH, Lammers CR, Reiss AL, Amaral DG (2004) The amygdala is enlarged in children but not adolescents with autism; the hippocampus is enlarged at all ages. J Neurosci 24: 6392–6401.

Schumann CM, Barnes CC, Lord C, Courchesne E (2009) Amygdala enlargement in toddlers with autism related to severity of social and communication impairments. Biol Psychiatry 66: 942–949.

Sparks BF, Friedman SD, Shaw DW, Aylward EH, Echelard D, Artru AA, Maravilla KR, Giedd JN, Munson J, Dawson G, Dager SR (2002) Brain structural abnormalities in young children with autism spectrum disorder. Neurology 59: 184–192.

Studholme C, Hill DLG, Hawkes DJ (1999) An overlap invariant entropy measure of 3D medical image alignment. Pattern Recognition 32: 71–76.

Suomi SJ, Mineka S, DeLizio RD (1983). Short- and long-term effects of repetitive mother-infant separations on social development in rhesus monkeys. Dev Psychol 19: 770–786.

Tai C, Chatziioannou A, Siegel S, Young J, Newport D, Goble RN, Nutt RE, Cherry SR (2001) Performance evaluation of the microPET P4: a PET system dedicated to animal imaging. Phys Med Biol 46: 1845–1862.

Talbot PS, Narendran R, Butelman ER, Huang Y, Ngo K, Slifstein M, Martinez D, Laruelle M, Hwang DR (2005) 11C-GR103545, a radiotracer for imaging kappa-opioid receptors *in vivo* with PET: synthesis and evaluation in baboons. J Nucl Med 46: 484–94.

Tan M, Parkin JE (2000). Route of decomposition of thiomersal (thimerosal). Int J Pharm 208: 23–34.

Tsang D, Ng SC, Ho KP, Ho WK (1982) Ontogenesis of opiate binding sites and radio-immunoassayable beta-endorphin and enkephalin in regions of rat brain. Brain Res 281: 257–261.

Van Bockstaele EJ, Rudoy C, Mannelli P, Oropeza V, Qian Y (2006) Elevated mu-opioid receptor expression in the nucleus of the solitary tract accompanies attenuated withdrawal signs after chronic low dose naltrexone in opiate-dependent rats. J Neurosci Res 83: 508–514.

Wamsley JK, Zarbin MA, Young WS, 3rd, Kuhar MJ (1982) Distribution of opiate receptors in the monkey brain: an autoradiographic study. Neuroscience 7: 595–613.

Wu X, Liang H, O'Hara KA, Yalowich JC, Hasinoff BB (2008). Thiol-modulated mechanisms of the cytotoxicity of thimerosal and inhibition of DNA topoisomerase II alpha. Chem Res Toxicol 21: 483–493.

Zagon IS, McLaughlin PJ, Weaver DJ, Zagon E (1982) Opiates, endorphins and the developing organism: a comprehensive bibliography. Neurosci Biobehav Rev 6: 439–479.

Zagon IS, McLaughlin PJ (1985) Naltrexone's influence on neurobehavioral development. Pharmacol Biochem Behav 22: 441–448.

Zagon IS, McLaughlin PJ (2004) Gene expression of OGFr in the developing and adult rat brain and cerebellum. Brain Res Bull 63: 57–63.